Adsorption and photocatalytic degradation of bisphenol A using TiO₂ and its separation by submerged hollowfiber ultrafiltration membrane

Jae-Wook Lee[1], Tae-Ouk Kwon[2], Ramesh Thiruvenkatachari[2], Il-Shik Moon[2,*]

(1. Department of Chemistry Engineer, Seonam University, Namwon 590-711, Korea; 2. Department of Chemistry Engineer, Sunchon National University, Suncheon 540-742, Korea. E-mail: ismoon@sunchon.ac.kr)

Abstract: This study evaluates the adsorption ability of bisphenol A(BPA) on titanium dioxide(TiO₂) and its effect on the photocatalysis by advanced oxidation process using UV radiation and TiO₂ photocatalyst. Degradation of BPA was also evaluated for the system without adsorption prior to photocatalytic reaction. The separation of TiO₂ from BPA solution treated by pilot-scale photocatalytic reactor (capacity 0.16 m³) was studied using submerged ultrafiltration (UF) membrane. It was found that although adsorption capacity of BPA was not high, adsorption played an important role in improving the efficiency of photocatalysis. On the other hand, during the separation of TiO₂ particles from aqueous suspension, the permeate flux of the membrane was strongly affected by transmembrane pressure and TiO₂ dose. The permeate turbidity was decreased below 1 NTU.

Keywords: bisphenol A; TiO₂; adsorption; membrane; photocatalysis

Introduction

Bisphenol A (2,2-bis(4-hydroxyphenyl) propane or BPA) is an important chemical compound used in various industries such as polycarbonate, polysulphone plastics, epoxy resins and unsaturated polyesterstyrene resins, reaction inhibitor, antioxidant in plastics, and flame retardant(Chiang et al., 2004). It is estimated that about 1 million tonnes of BPA is produced in the U. S. each year and in the EU alone, in 1997/1998, annual consumption of BPA was estimated at approximately 640000 t (640 × 10⁶ kg) (Lyons, 2000). The global production is reported to be increasing at about 7% per year. However, a recent report by the European Commission DG ENV(2000) and others (Lyons, 2000; Schafer et al., 1999) have revealed the endocrine disrupting effects of BPA. BPA is known to exhibit estrogenic activity and alter metabolism, induce DNA damages and result in chromosomal aberrations. Hence, considering the widespread application of BPA with its high risk of exposure and health hazard, there is a strong need for a suitable and effective remediation treatment technology for the destruction of BPA from water.

Many treatment methods have been investigated using chemical, biological, photochemical and electrochemical procedures (Al-Bastaki, 2004). Conventional biological methods for the removal of pollutants in wastewater require longer time, and simple chemical oxidation alone cannot completely eliminate these organic compounds (Al-Bastaki, 2004; Ohko et al., 2001). Recently, advanced oxidation processes (AOPs) have attracted much attention in the pro-duction and utilization of hydroxyl radicals, which serves as a powerful oxidant for organic destruction. To generate the hydroxyl radicals, ozone, hydrogen peroxide and UV radiation have been used. Recently, UV with suspended TiO₂ particles is one of the most promising techniques for producing hydroxyl radicals because of many advantages including high photocatalytic activity, high stability, non-environmental impact and low cost (Al-Bastaki, 2004). Many studies have been reported on the mechanism of photocatalytic degradation of BPA in small-scale apparatus (Ohko et al., 2001; Kaneco et al., 2004). However, little work has been done to investigate the influence of adsorption prior to the photocatalysis.Another aspect in photocatalytic oxidation is that, TiO₂ catalysts are either suspended as a slurry in the water or fixed (i.e., immobilized) on a supporters such as glass, concrete and ceramics (Tennakone et al., 1997; Kaneco et al., 2004; Xi and Geissen, 2001). But the latter method has some drawbacks such as limiting mass transfer and a loss of photocatalytic activity. Thus, slurry type reactor system is more superior that catalyst immobilized photo oxidation in terms of photocatalytic degradation efficiency (Lee et al., 2001). However, TiO₂ particles have to be separated from the treated water in slurry reactors after the photocatalytic degradation. A major difficulty in the separation of TiO₂ particles is that it is too fine(with an average primary particle size of about 21 nm) to be removed from suspension by mere sedimentation. Recently, some attempts have been made to cleaned effectively separate TiO₂ particles by membrane filtration (Xi and Geissen, 2001; Lee et al., 2001). Xi

and Geissen(2001) have studied the separation of TiO$_2$ from photocatalytically treated water by cross-flow microfiltration membrane.

The main objective of the study was to investigate the effect of adsorption on photocatalytic degradation of BPA using TiO$_2$ as photocatalyst. Submerged UF membrane process was adopted for the separation of TiO$_2$ after photocatalysis.

1 Experimental

The BPA used in this study was purchased from Junsei Chemical Co., Ltd., Japan. Aqueous solution of BPA was prepared with distilled water. P-25 TiO$_2$ particles(Degussa, Germany) were used as adsorbents and/or photocatalysts. The nitrogen adsorption apparatus (ASAP 2010, Micromeritics, USA) was used to measure the surface area and pore size distribution. Particle size distribution of TiO$_2$ was analyzed using particle size analyzer (ASAP 2010 Micropore, Micromeritics, USA). The physiochemical properties of TiO$_2$ are listed in Table 1. The adsorption equilibrium experiments were carried out by contacting a given amount of TiO$_2$ with BPA solution of concentration ranging from 1—100 mg/L, in a constant temperature (25℃) shaking incubator. Solution pH was adjusted using HCl and NaOH. Three days of thorough mixing was carried out in order to reach equilibrium. Then the solution was analyzed using high performance liquid chromatography (Shimadzu LC-10 VP, Japan) after filtering the sample with a 0.015 μm UF membrane filter, in order to check the residual BPA concentration. The adsorption capacity (q) of TiO$_2$ was determined from material balance using the following expression:

$$q = \frac{V(C_0 - C)}{m} \qquad (1)$$

where, C_0 and C are the initial and equilibrium (or residual) liquid-phase concentrations (mg/L), respectively; V is the volume of solution (L); and m is the weight of dry TiO$_2$(mg). On the other hand, adsorption kinetic experiments were conducted in a Carberry-type batch adsorber in order to obtain concentration decay curves as a function of time.

In the photocatalytic process, solutions of 10 to 100 mg/L BPA (initial) concentration and 1 g/L of TiO$_2$ as photocatalysts were used. The TiO$_2$ suspension containing BPA was irradiated in the photocatalytic reactor using 6 quartz tube mercury vapor lamps (TUV 36 SP T5, Philips, USA) with a power input of 40 W. The irradiation intensity was 144 μW/cm^2 and the wavelength was 253.7 nm. The effective volume of the liquid within the reactor was
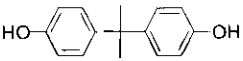
Table 1   Physico-chemical properties of TiO$_2$.

Property	Value
Surface area(BET), m^2/g	50[a](43.2[b])
Surface area(Astakov), m^2/g	62.4[b]
Pore volume, cm^3/g	0.19[b]
Average pore size, nm	6.9[b]
Average particle size, nm	Approx.21[a,b]
Density, g/L	Approx.130[a]
Purity, %	>99.5[a]
Supplier, Degussa	P25

Notes: [a] Manufacturer's report; ' size of the primary particles;
[b] measured in this work

130 L. TiO$_2$ in aqueous solution was kept in suspension in the reaction vessel using a circulation pump, without any temperature control. The amount of BPA in the aqueous solution was measured by total organic carbon analyzer(Shimadzu 500A, Japan) and a high-performance liquid chromatography (Shimadzu LC-10 VP, Japan) equipped with a UV detector (Shimadzu SPD-10A VP) and a Shim-pack CLC-ODS column. The elution was monitored at 275 nm. The elutant used was a solvent mixture of methanol and water(7:3, v/v). The flow rate of the mobile phase was 1 ml/min. The TiO$_2$ photocatalyst was removed from the solution by filtration, and the resulting solution was analyzed with HPLC. The experimental conditions for the photocatalytic degradation of BPA are listed in Table 2. For the analysis of intermediate products, a GC/MS (Shimadzu QP2010, Japan) equipped with HP-5 capillary column (30 m ×0.25 mm i.d) was used according to the procedure reported by Kaneko *et al.* (2004).

Table 2   Experimental conditions

BPA chemical structure	HO—⟨◯⟩—⟨◯⟩—OH
BPA concentration	10—100 mg/L
TiO$_2$ concentration	200—1000 mg/L
Temperature	35—70℃
pH	2—9
Light intensity per lamp	144 μW/cm^2
Illumination time	25 h

A submerged hollow fiber UF membrane was used for TiO$_2$ particle separation from water. The membrane was polysulfone UF(Kolon, Korea) with an effective surface area of 0.7 m^2. Membranes were cleaned with distilled water prior to the experiment. The important properties of the membrane are listed in Table 3. The UF unit consists of a vaccum pump, a submerged hollow fiber membrane, pressure gauge, flow meter and feed and permeate tanks. The

experimental data were obtained at different operating pressures (150, 200, 250 mmHg) and TiO_2 amounts (0.2—3.0 g/L).

Fig.1 shows a schematic diagram of the combined treatment process, which consists of adsorption chamber, photocatalytic reactor followed by submerged hollow UF membrane.

Table 3 Specifications of submerged UF hollow fibemebrane

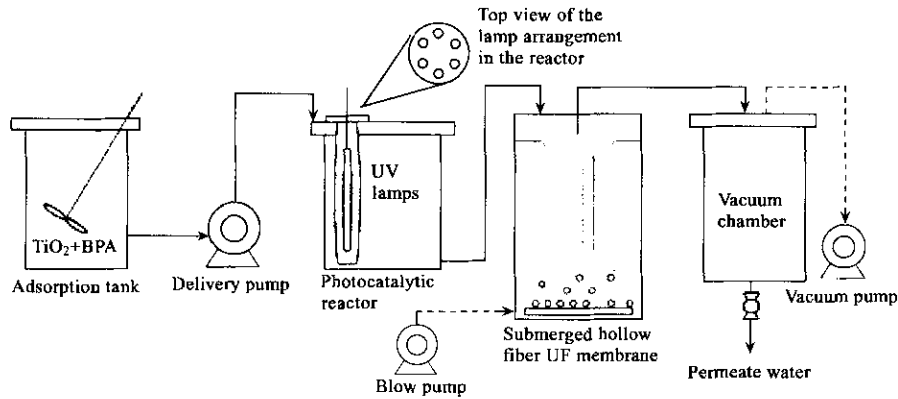| Material	Polysulfone
Pore size, μm	0.015
Surface area, m^2	0.7
Element length, mm	415
Element diameter, mm	2
Feed temperature, ℃	<40
Operating pressure, mmHg	100—300
Operating pH	6

Fig.1 Schematic diagram of a lab-scale adsorption-photocatalysis-ultrafiltration system

2 Results and discussion

2.1 Adsorption studies

Prior to adsorption studies, important physical properties of TiO_2 were determined. The surface area and pore size distribution of a sorbent significantly affect the adsorption behavior (Ruthven, 1984; Yang, 1986; Lee et al., 1997, 2004a, 2004b). The surface area and pore size distribution of TiO_2 were measured using nitrogen adsorption isotherm. The surface area was found to be small at about 43.2 m^2/g. The average pore determined from the BJH (Barrett, Joyner and Halenda) method was about 6.9 nm. The results are listed in Table 1. As shown in Fig.2, TiO_2 has somewhat broader distribution from 2 to 400 nm.

Adsorption onto porous sorbent is generally driven by the dispersed forces between the sorbate and the sorbent. Besides, the adsorption capacity is also influenced by other factors such as temperature and pH of the solution. Fig.3 shows the adsorption isotherms of BPA on TiO_2 at 25℃ in the absence of light. The adsorption capacity of 100 mg/L of BPA was approximately 60 mg/g. The solid lines in Fig.3 are the predicted results with Langmuir, Freundlich and Sips isotherms.

Langmuir $q = \dfrac{q_m bC}{1+bC}$ (2)

Freundlich $q = kC^{1/n}$ (3)

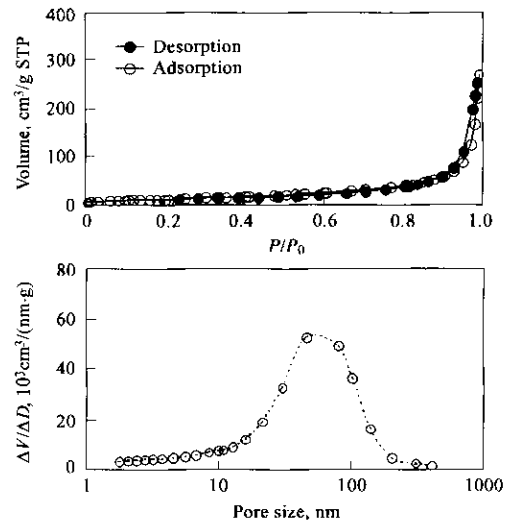Sips $q = \dfrac{q_m bC^{1/n}}{1+bC^{1/n}}$ (4)

Fig.2 Nitrogen adsorption and desorption isotherms and pore size distribution

Among the isotherms, Langmuir and Sips models were found to satisfactorily describe the adsorption of BPA. The isotherm parameters were determined by minimizing the mean percentage deviations between experimental and predicted amounts adsorbed, based on a modified Levenberg-Marquardt method (IMSL routine DUNSLF). The object function, E (%), represents the average percentage deviation between experimental and predicted results as follows:

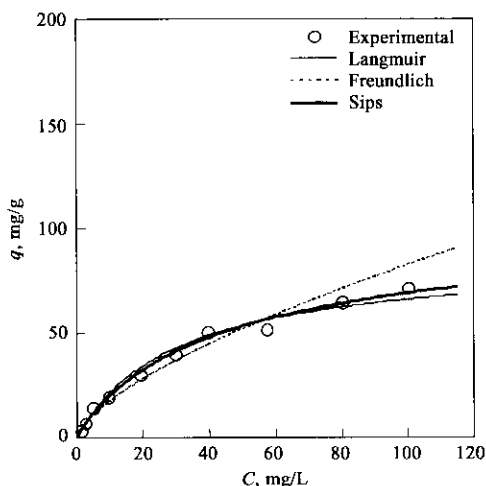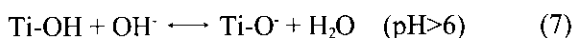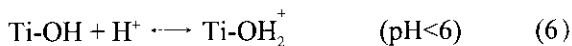$$E(\%) = \frac{100}{n} \sum_{k=1}^{n} \left[\frac{|q_{exp,k} - q_{cal,k}|}{q_{exp,k}} \right]   (5)$$

Fig.3   Adsorption isotherm of BPA on TiO$_2$particles at 25°C without UV illumination

Here, n is the number of experimental data; $q_{exp,i}$ is the experimental adsorption capacity; and $q_{cal,i}$ is the calculated adsorption capacity. The determined isotherm parameters were listed in Table 4. The values of q_m and b for Langmuir isotherm were 86 mg/g and 0.034 L/mg, respectively. A similar result was obtained by Ohko *et al.*(2001).

Table 4   Isotherm parameters of BPA

Isotherms	Parameters	Values
Langmuir	q_m	0.860×10^2
	b	0.034
	$E(\%)$	6.14
Freundlich	k	3.992
	n	1.517
	$E(\%)$	12.67
Sips	q_m	1.049×10^2
	b	0.031
	n	1.106
	$E(\%)$	5.08

Among various operating parameters affecting adsorption capacity in liquid-phase adsorption, pH is the most important factor. Fig. 4 shows the effect of initial pH (2, 3, 4, 6, 7, 9) on adsorption capacity of BPA. Results showed that the adsorption capacity was the highest (57.6 mg/g) around the isoelectric point. The zero point charge (i.e., isoelectric point) of TiO$_2$ particles is around 6(Kaneco *et al.*, 2004). It has been known that the surface of TiO$_2$ is covered with hydroxyl groups as well as molecular water in aqueous solution. The surface charge of the TiO$_2$ photocatalyst shows amphoteric behavior depending on the solution pH. From the surface acid-base equilibrium relationship, it can be written as follows:

$$\text{Ti-OH} + \text{H}^+ \longrightarrow \text{Ti-OH}_2^+ \qquad (\text{pH}<6) \qquad (6)$$

$$\text{Ti-OH} + \text{OH}^- \longrightarrow \text{Ti-O}^- + \text{H}_2\text{O} \quad (\text{pH}>6) \qquad (7)$$

Thus, TiO$_2$ surface is positively charged in acidic condition (pH<6) and it is negatively charged under alkaline condition (pH>6). Our experimental results revealed that there was no significant effect of pH in the range of 2 to 9 on the adsorption capacity of BPA on TiO$_2$ as shown in Fig.4. Consequently, pH 6 was chosen as the optimal condition for the adsorption of BPA. The adsorption capacity of BPA on TiO$_2$ was determined at different solution temperatures (Fig.5). Results indicated that adsorption capacity gradually decreased from 20.34 to 14.54 mg/g as the temperature increased from 25 to 65°C.

The determination of external and internal mass transfer coefficients within TiO$_2$ sorbent is an important task for the design and scale-up of large-scale processes. Internal mass transfer is usually the rate-controlling step in most adsorption processes (Yang, 1986; Ruthven, 1984). In this work, the surface diffusion model was chosen to describe internal mass transfer within porous TiO$_2$ particles.
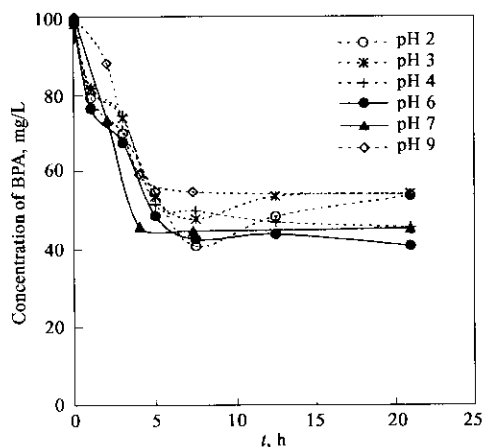

Fig.4   Adsorption capacity of BPA on TiO$_2$ in terms of initial pH range of 2 - 9 without UV illumination
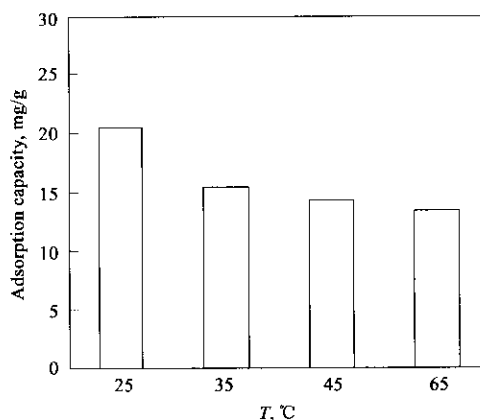

Fig.5   Adsorption capacity of BPA on TiO$_2$ in terms of temperature without UV illumination

$$\frac{\partial q_i}{\partial t} = D_{si} \left(\frac{\partial^2 q_i}{\partial r^2} + \frac{2}{r} \frac{\partial q_i}{\partial r} \right) \quad (8)$$

Detailed descriptions on the diffusion model equations and numerical technique to solve model equations are given elsewhere (Lee *et al.*, 2004a, 2004b). Among various methods for determining the mass transfer coefficient, the most general method is to compare the experimental concentration decay curves and the predicted values using the specified model. Fig.6 illustrates the concentration decay curves of BPA on TiO₂ in a batch adsorber. The solid line is the predicted results by employing surface diffusion model. The external and internal diffusivities determined were 3.92×10^{-7} m/s and 1.07×10^{-15} m²/s, respectively. Results indicated that the values of two diffusivities for powder form of TiO₂ were considerably low. More than 21 h was required to achieve adsorption equilibrium of BPA on the TiO₂ photocatalyst at 25℃.

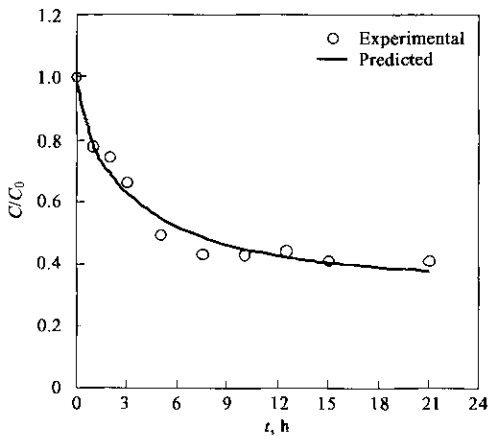Fig.6　Concentration decay curve of BPA in a batch adsorber at 25℃ (shaking 200 r/min, 1 L of 100 mg/L BPA, TiO₂ dose 1 g; pH 6) without UV illumination

2.2 Photocatalytic degradation studies

The reactor temperature in the photocatalytic reactor increased from 35 to 70℃ , within the experimental time of 24 h. Kaneko *et al.*(2004) studied the effect of various factors, such as photocatalyst dosage, initial substrate concentration, temperature, pH and light intensity, on the photocatalytic degradation of BPA for the complete degradation. The study indicated that the photocatalytic system was not so sensible to temperature because the photonic activation occurs at considerably high speed. Hence the temperature was not controlled during this study period.

Fig.7 shows the effect of typical substrate concentration (10, 50 and 100 mg/L) on the photocatalysis of BPA using TiO₂. Experimental

results showed that BPA was almost completely decomposed within 5 h at lower concentration(10 mg/L) while a gradual degradation pattern was observed for higher BPA concentration(100 mg/L). In other words, higher degradation efficiency was noted at lower initial concentration. For example, 50% of initial BPA was decomposed within 1 h, 9 h and 24 h at 10, 50 and 100 mg/L initial concentration, respectively.
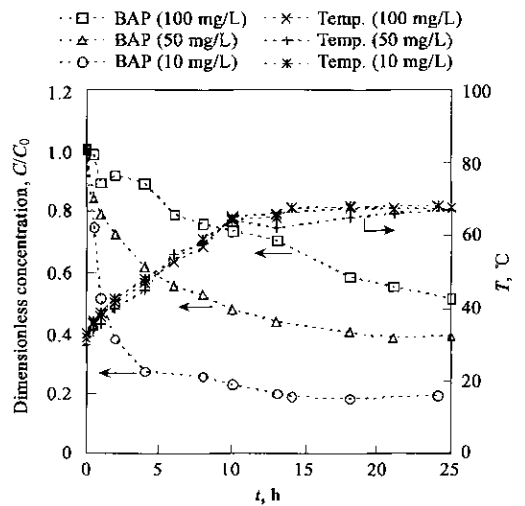

Fig.7　Effect of BPA concentrations (10, 50, 100 mg/L) on photocatalytic degradation using TiO₂
(TiO₂: 1 g/L, 150 L of BPA; pH 6, light intensity: 144 μW/cm²)

It has been known that the photocatalytic degradation reaction of BPA follows a pseudo-first-order kinetic law and its kinetics may be expressed as follows(Kaneco *et al.*, 2004; Gao *et al.*, 2003):

$$r = -\frac{dC}{dt} = kC^n \quad (9)$$

where k is the reaction rate constant; n is the reaction order; and C is the reaction concentration of BPA. A straight line was obtained by plotting $\ln \left(-\frac{dC}{dt} \right)$ vs. $\ln C$ in the concentration range of 10 to 100 mg/L at pH 6. The reaction rate and order determined from the intercept and slope of the straight line were 0.052 and 0.81, respectively.

Pretreatment of BPA adsorption on TiO₂ played a crucial role in photocatalytic degradation efficiency. Prior to photodegradation experiments, the suspension was stirred for more than 26 h in the dark to achieve adsorption equilibrium of BPA on TiO₂ catalyst at an initial reactor temperature of 35℃ . Then, UV irradiation was introduced without controlling the temperature of the reactor. More than 95% of the initial BPA(10 mg/L) concentration was degraded within 5 h of UV irradiation following the first-order kinetics. However, 80% removal efficiency can be observed without adsorption process prior to photocatalytic

degradation experiment. Fig.8 shows the BPA degradation efficiency for the photocatalytic reactor with and without adsorption pretreatment. The increase in temperature with time inside the reactor is also shown in the Fig. 8.
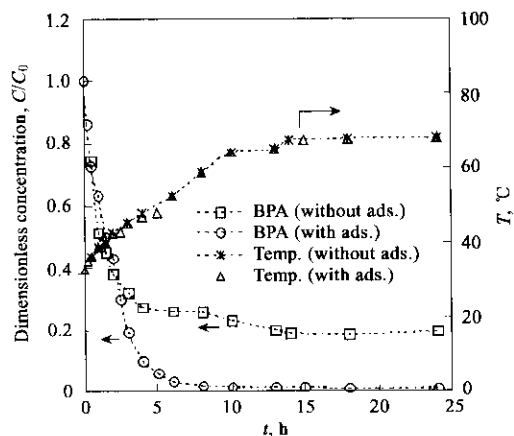

Fig.8 Photocatalytic degradation of BPA with and without adsorption prior to photocatalytic reaction
Adsorption time 16 h, shaking 200 r/min, 150 L of 10 mg/L BPA, pH 6, TiO₂ 1 g/L, light intensity 144 μW/cm²

Intermediate organic products formed in the UV photocatalytic degradation with 10 mg/L of initial BPA concentration in the aqueous TiO₂ suspension were identified by GC/MS analysis. In the photo-catalytic degradation of BPA with TiO₂, various intermediate products including phenol, *p*-hydroquin-one, *p*-isopropenylphenol, *p*-hydroxybenzaldehyde and 4-hydrozyphenyl-2-propanol were confirmed by several researchers on the basis of peaks of GC-MS chromatogram(Horikoshi *et al.*, 2004; Fukahori *et al.*, 2003). Each peak obtained from GC-MS chromato-gram, was identified by comparing with GC-MS WILEY7 library data. The formation of similar intermediate products was also reported by Ohko *et al.* (2001) during the photocatalytic degradation of BPA using TiO₂. Examining the GC-MS chromatogram results, it was evident that as time progressed the initial peak representing BPA, gradually reduced and corresponding smaller peaks, representing the for- mation of intermediates, appeared and disappeared. It can be understood that the aromatic intermediates formed presumably were further oxidized to aliphatic compounds and finally mineralized to carbon dioxide. On the basis of experimental results obtained from this study, it was found that the TiO₂ photocatalysis is a useful technology for the water treatment containing BPA without generating any serious secondary pollution.

2.3 Membrane separation studies

In order to obtain reusable quality treated water

and to recover the used TiO₂ for possible reuse, submerged UF membrane was applied as a final step for the separation of TiO₂ from BPA solution treated by pilot-scale photocatalytic reaction. In spite of many advantages of membranes, the application of mem-brane process for particle separation has been limited because of the flux decline resulting mainly from fouling of the pores of the membrane(Mulder, 1996; Murthy and Gupta, 1999). Fouling is a complex phenomenon with many influencing factors including the membrane pore plugging, chemical degradation, and concentration increase of contaminants including bacteria, organic and inorganic materials near the membrane surface. When particle is a major foulant, the understanding of interaction between particles, or between particle and membrane surface is very impor-tant because it has a significant influence on the separation efficiency of membrane filtration. In addition, the flux decline resulting from fouling depends on the physical and chemical parameters of the solution to be treated such as concentration, temperature, pH, ionic strength and specific inter-actions(hydrogen bonding, dipole-dipole interactions). On the other hand, a decrease in particle size in a finely dispersed suspensions result in an increase in the interfacial effects. TiO₂ particles tend to aggregate near its isoelectric point, whereas particles with a higher surface charge are well dispersed. It has been known that the maximum particle size was observed around isoelectric point of TiO₂. This behavior was explained based on the fact that the repulsion forces and the distance between the particles increases with the magnitude (either positive or negative) of the zeta-potential(Xi and Geissen, 2001). In this study, the flux decline of submerged UF membrane was examined under two operating conditions, namely, TiO₂ amounts(0.2, 1, 2, 3 g/L) and permeate pressures (150, 200, 250 mmHg) at constant pH 6 (isoelectric point), as shown in Fig.9. Continuous flux decline may come from membrane fouling mainly due to the deposition of TiO₂ particles on the membrane. This includes adsorption, pore blocking, precipitation and cake formation. Experimental permeate flux in terms of different permeate pressures obtained in this work was in the range of 192 to 127 L / (m²·h) at the initial stage. At high permeate pressures the particle deposition rate was enhanced with the increase in the permeate flux, thereby causing an increase in the accumulation of particles in the cake layer. The opti-mum operating pressure is a function of the process conditions and can be determined by cost opti-mization.
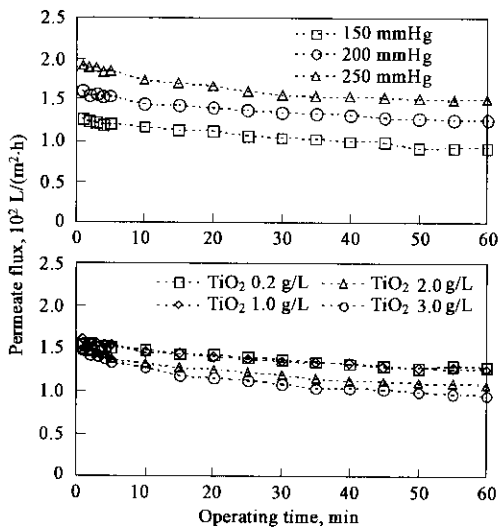
Fig.9 Flux decline in terms of (a) TiO₂ dosage and (b) operating pressure at pH 6

On the other hand, the flux decline was not highly sensitive to TiO₂ dose of 0.2 to 1 g/L. However, when TiO₂ particles over 2 g/L were used, there was a noticeable flux decline from 150 to 120 L/(m²·h)(corresponding to a reduction of approximately 20%) during 1 h of operation. This result implies that one should be very careful in determining the optimal TiO₂ dose by considering the photocatalytic reaction as well as UF separation efficiency of TiO₂. Under the experimental conditions of 1.0 g/L TiO₂ and 200 mmHg permeate pressure applied, permeate fluxes of up to 140 L/ (m²·h) can be obtained. Xi and Geissen (2001) investigated systematically the effect of various operating variables, including flow velocity, transmembrane pressure and feed concentration, pH of the suspension and electrolyte concentration, on permeate flux of cross-flow microfiltration, for TiO₂ suspension. Their results also proved that during the separation of TiO₂ particles, controlling the coag- ulation state of TiO₂ particles at pH close to the isoelectric point gave higher flux. The performance of UF submerged membrane on the separation of TiO₂ particles in terms of turbidity was investigated. The initial and the treated water turbidities were 3929 NTU and 0.7 NTU, respectively. This indicates that almost 99.9% of TiO₂ particles were separated from the solution by the UF membrane(pore size about 0.015 μm) without any form of pretreatment.

The particle cake on the membrane surface eventually reached a steady-state when the particle convection to the cake surface was balanced by the back-transport of the particles away from the surface of the cake layer(Lee et al., 2001). Belfort et al.(1994) investigated the influence of particle size on deposit

rate on membrane surface. They found that the larger particles deposited selectively on the filter surface at faster rates than the finer particles. The particle size distributions for a mixture of TiO₂ and BPA (TiO₂ 1 g/L, BPA 10 mg/L, pH 6) were measured using a particle size analyzer. The result indicated that the particles have wide size distribution in the range of 0.1 to 1.0 μm. This result implies that the TiO₂ particles form aggregates in water because TiO₂ are very fine with an average primary particle size of about 21 nm. From this result, submerged UF membrane with average pore size of 0.015 μm (Table 2), seems to be suitable for the separation of TiO₂ from aqueous solution.

3 Conclusions

A pilot-scale photocatalytic reactor (0.16 m³) comprising of adsorption process as the pre-treatment and submerged UF membrane system with a processing capacity of 1.44 m³/d as the post-treatment, for BPA degradation and TiO₂ separation, was evaluated. Adsorption isotherm data fitted well using Langmuir and Sips equations. There was no significant effect of pH on adsorption capacity. The external and internal diffusivities of BPA on TiO₂ sorbent were 3.92×10^{-7} m/s and 1.07×10^{-15} m²/s, respectively. Although adsorption capacity of BPA was not high, adsorption played an important role in improving the efficiency of photocatalysis. More than 95% of the initial BPA(10 mg/L) concentration was degraded within 5 h of UV irradiation following the first-order kinetics. However, 80% removal efficiency can be observed for the system without adsorption prior to photocatalytic degradation experiment. This could lead to the reduction of amount of TiO₂ dose, which would also reduce the burden on the post treatment using submerged UF membrane. Results from TiO₂ separation revealed that the flux decline of submerged UF was highly sensible to the operating conditions such as transmembrane pressure and TiO₂ dose. Under the experimental conditions of 1.0 g/L TiO₂ and 200 mmHg permeate pressure, permeate fluxes of up to 140 L/(m²·h) was obtained. The permeate turbidity of 0.7 NTU was achieved. On the basis of our experimental results, it was also found that the submerged UF is potentially an attractive process for the separation of TiO₂ from photocatalytically treated BPA solution.

References:

Al-Bastaki N M, 2004. Performance of advanced methods for treatment of wastewater: UV/TiO₂, RO and UF [J]. Chem Eng and Process,

43: 935—940.

Belfort G, Davis R H, Zydney A L, 1994. The behavior of suspensions and macromolecular solutions in crossflow microfiltration [J]. Membr Sci, 96: 1—58.

Chiang K, Lim T M, Tsen L *et al.*, 2004. Photocatalytic degradation and mineralization of bisphenol A by TiO_2 and platinized TiO_2 [J]. Appl Catal A: General, 261: 225—237.

European Commission DG ENV, 2000. Towards the establishment of a priority list of substances for further evaluation of their role in endocrine disruption-preparation of a candidate list of substances as a basis for priority setting[Z]. BKH Consulting Engineers.

Fukahori S, Ichiura H, Kitaoka T *et al.*, 2003. Capturing of bisphenol a photodecomposition intermediates by composite TiO_2-zeolite sheets[J]. Appl Catal B: Environ, 46: 453—462.

Gao Y, Chen B, Li H *et al.*, 2003. Preparation and characterization of a magnetically separated photocatalyst and its catalytic properties [J]. Materials Chemistry, 80: 348—355.

Horikoshi S, Tokunaga A, Hidaka H *et al.*, 2004. Environmental remediation by an integrated microwave/UV illumination method: VIL Thermal/non-thermal effects in the microwave-assisted photocatalyzed mineralization of bisphenol A [J]. Photochem Photobiol A: Chem, 162: 33—40.

Kaneco S, Rahman M A, Suzuki T *et al.*, 2004. Optimization of solar photocatalytic degradation conditions of bisphenol A in water using titanium dioxide [J]. Photochem Photobiol A: Chem, 163: 419—424.

Lee J W, Park H C, Moon H, 1997. Adsorption and desorption of cephalosporin C on nonionic polymeric sorbents [J]. Sep and Purif Tech, 12: 1—11.

Lee S A, Choo K H, Lee C H *et al.*, 2001. Use of ultrafiltration membrane for the separation of TiO_2 photocatalysts in drinking water treatment[J]. Ind Eng Chem Res, 40: 1712—1719.

Lee J W, Kwon T O, Moon I S, 2004a. Adsorption of monosaccharides, disccharides, and maltooligosaccharides on activated carbon for separation of maltopentaose[J]. Carbon, 42: 371—380.

Lee J W, Shim W G, Ko J Y *et al.*, 2004b. Adsorption equilibria, kinetics, and column dynamics of chlorophenols on a nonionic polymeric sorbent XAD-1600 [J]. Sep and Sci Tech, 39: 2041—2065.

Lyons G, 2000. Bisphenol A: A known endocrine disruptor [R]. WWF European Toxics Programme Report, UK.

Mulder M, 1996. Basic principles of membrane technology [M]. The Netherlands: Kluwer Academic Publishers: Dordrecht.

Murthy Z V P, Gupta S K, 1999. Sodium cyanide separation and parameter estimation for reverse osmosis thin film composite polyamide membrane[J]. Membr Sci, 154: 89—103.

Ohko Y, Ando I, Niwa C *et al.*, 2001. Degradation of bisphenol A in water by TiO_2 photocatalyst[J]. Envoron Sci Technol, 35: 2365—2368.

Ruthven D M, 1984. Principles of adsorption and desorption processes [M]. New York: John Wiley & Sons.

Schafer T, Lapp C, Hanes C *et al.*, 1999. Estrogenicity of bisphenol A and bisphenol A dimethacrylate *in vitro* [J]. Biomed Mater Res, 45: 192—197.

Tennakone K, Tilakaratne C T K, Kottegoda I R M, 1997. Photo-mineralization of carbofuran by TiO_2-supported catalyst [J]. Wat Res, 31: 1909—1912.

Xi W, Geissen S U, 2001. Separation of titanium dioxide from photocatalytically treated water by cross-flow microfiltration[J]. Wat Res, 35: 1256—1262.

Yang R T, 1986. Gas separation by adsorption processes [M]. Boston: Butterworths.